Effect of Polymerization Conditions on the Melt Rheological Properties of Vinyl Chloride–Vinyl Acetate Copolymers

MICHAEL LANGSAM and JOHN T. CHENG, *Air Products and Chemicals, Inc., Allentown, Pennsylvania 18105*

Synopsis

Mathematical models have been developed which predict the composition, molecular weight, and melt rheological properties for vinyl chloride/vinyl acetate copolymers of inherent viscosity range 0.4–0.7 dL/g and bound vinyl acetate levels of 3.8–17.4%. The effect of polymer long chain branching on the viscous/elastic moduli ratio is discussed as well as the comparison of Tinius–Olsen melt index measurements vs. mechanical spectrometer results. The reactivity ratio for vinyl chloride/vinyl acetate comonomer pairs was remeasured and found to be significantly different from literature values.

INTRODUCTION

The vinyl chloride–vinyl acetate copolymers have a wide range of applications and are the largest volume copolymers of vinyl chloride.[1] These copolymer resins are most frequently fabricated by thermal processes: calendering for film and sheet applications and compression molding for audio phonograph record applications. The relationship between the polymerization process and the structure of the copolymer formed will affect the thermal fabrication of these resins. In order to use these copolymer resins most effectively in different applications, it is important to understand how the polymerization process affects the polymer structure and how this in turn will affect the thermal fabrication processes.

The relationship between polymerization conditions and the subsequent structure for the homopolymer of vinyl chloride has been well established.[2] In addition, the relationship between the homopolymer structure and melt rheology has also been quantified.[3–5] Therefore the relationship between the polymerization conditions and polymer melt rheology is readily determined for the homopolymers of vinyl chloride. By contrast, these data are not readily available for the copolymer of vinyl chloride vinyl acetate. Chen and Blanchard[6] reported the results of a fractionation study of an 85/15 vinyl chloride/vinyl acetate copolymer. They found an extremely wide range in the number average molecular weight between each of the fractions. Janca and co-workers[7–9] have extended these fractionation studies to include several copolymers with different vinyl chloride/vinyl acetate ratios. They also demonstrated that as the vinyl acetate content of each of the fractions increases the molecular weight decreases. Recently, Mori[10] has reported the development of a dual detector gel permeation chromatography device which measures simultaneously the molecular weight and the com-

Journal of Applied Polymer Science, Vol. 30, 1285–1308 (1985)
 CCC 0021-8995/85/031285-24$04.00

position of a vinyl chloride/vinyl acetate copolymer. His analytical results confirmed the previously described work of Janca and co-workers.

The variations in vinyl acetate content as a function of conversion[11] and the presence of long chain branching[12] in the vinyl chloride/vinyl acetate copolymers offer an opportunity to determine how polymer structure can affect the melt rheology.

A series of vinyl chloride/vinyl acetate copolymers were prepared to fit a 4 × 4 matrix of bound vinyl actate (VacB) and inherent viscosity (IV) values. These values ranged from VAcB levels of approximately 4%, 8%, 12%, and 16% and IV values of approximately 0.4, 0.5, 0.6 and 0.7 dL/g. A total of 16 resins were prepared for this study. These are detailed in Table I. The VAcB level was controlled by varying the charged vinyl acetate (VAcC) level and carrying the polymerizations to a constant conversion. The IV of the copolymer was controlled by varying the polymerization temperature and the level of trichloroethylene chain transfer agent. Previous experience had shown that vinyl acetate would act as a chain transfer agent relative to vinyl chloride, and therefore we would require a reduction in the polymerization temperature (comparison of run 10 vs. run 14—Table I) to achieve a particular IV at higher vinyl acetate levels. In this study we chose the following experimental constraints:

1. Initiator level such that a 4–5-h polymerization cycle was achieved.
2. Initiator type was varied so as to achieve a reasonable polymerization kinetic profile over the range of polymerization temperature. Lauroyl peroxide was used from 55°C to 65°C; azobisisobutyronitrile was used from 67.5°C to 73°C.
3. A maximum polymerization temperature of 73°C was used because of the laboratory reactor pressure rating.

TABLE I
Experimental Vinyl Acetate–Vinyl Chloride Copolymers; Synthesis and Physical Properties

Experiment no.	VAcC (%)	T_p (°C)	TCE (phm)	Level/type[a] (PHM)		MF (g/10 mm)	VacB (%)	IV (dL/g)	Yield (%)
1	5.0	62.5	0	0.16	L	0.6	4.4	0.725	87.2
2	5.0	70	0	0.07	A	2.6	3.8	0.587	84.0
3	5.0	73	0.88	0.05	A	29.0	3.8	0.501	86.5
4	5.0	73	2.20	0.065	A	109.0	3.8	0.414	87.9
5	10.0	60	0	0.20	L	3.4	8.2	0.707	87.6
6	10.0	67.5	0	0.04	A	14.0	8.0	0.609	87.3
7	10.0	73	0.43	0.05	A	65.0	8.1	0.495	84.4
8	10.0	73	1.71	0.06	A	210.0	8.1	0.419	83.5
9	15.0	57.5	0	0.15	L	8.0	12.4	0.716	87.7
10	15.0	65	0	0.10	L	26.0	12.1	0.616	86.6
11	16.2	73	0.24	0.05	A	118.0	12.9	0.492	87.3
12	16.2	73	1.43	0.065	A	303.0	12.9	0.410	82.9
13	20.0	55	0	0.15	L	11.6	17.4	0.730	91.8
14	20.0	62.5	0	0.11	L	36.0	16.7	0.617	89.0
15	20.0	73	0.14	0.05	A	151.0	16.5	0.489	84.3
16	20.0	73	1.37	0.065	A	387.0	16.8	0.401	85.2

[a] A ≡ azobis[isobutyronitrile]; L ≡ Lauroyl peroxide.

TABLE II
Effects of Variations in Polymerization Temperature and Trichloroethylene Content on Copolymer Composition[a]

Run no.	Polymerization time (hr)	Yield (%)	VAcB (%)	IV (dL/g)
Series 1: olymerization temperature = 70°C				
	trichloroethylene level = 0 phm			
	AIBN level = 0.10 phm			
17A	4	91.4	12.7	0.556
B	2	45.2	9.8	0.541
C	1	17.5	8.4	0.535
D	½	8.4	8.2	0.524
Series 2: polymerization temperature = 70°C				
	trichloroethylene level = 0.366 phm			
	AIBN level = 0.12 phm			
18A	4	89.3	12.6	0.527
B	2	42.2	9.1	0.521
C	1	18.4	8.4	0.518
D	½	8.5	7.8	0.516
Series 3: polymerization temperature = 65°C				
	trichloroethylene level = 0 phm			
	Lauroyl peroxide level = 0.18 phm			
19A	4	87.6	12.2	0.673
B	2	53.5	9.7	0.652
C	1	22.9	8.4	0.643
D	½	10.0	7.9	0.618

[a] Recipe (same as under Experimental): vinyl chloride 85, vinyl acetate 15, initiator/trichloroethylene/polymerization temperature as indicated.

Prior to the start of these experiments, it was necessary to establish that the composition of the copolymer would not be affected by experimental variables such as polymerization temperature, initiator type and level, or the use of trichloroethylene chain transfer agent. These are detailed in Tables II and III. In addition we established that within our experimental study variations in the suspension agent level (from 0.10 to 0.30 phm) and reactor agitation (300–800 rpm) had no effect on the copolymer composition or on the inherent viscosity by partition effects between the comonomer phase and the aqueous phase. The particle properties of the copolymer resin were affected greatly by the agitation and level of suspending agent.

TABLE III
Effect of Trichloroethylene Constant on Conversion and Copolymer Composition[a]

Run no.	Trichloroethylene (phm)	Polymerization time (h)	Yield (%)	VAc(B) (%)	IV (dL/g)
20	0	3.25	89.2	12.5	0.494
21	0.366	3.75	90.4	12.4	0.464
22	0.732	4.00	87.6	12.8	0.423
23	1.46	4.25	88.4	12.5	0.396

[a] Vinyl chloride 85; vinyl acetate 15; AIBN 0.13; polymerization temperature 73°C; termination point, 95 psig pressure drop.

EXPERIMENTAL

Materials

Water. tap water passed through a deionizing column and then distilled under a nitrogen purge.

Suspending agent. commercial polyamide material.

Initiator. Lauroyl peroxide frm Lucidol, used as received. Azobisisobutyronitrile (AIBN) from DuPont Corp., used as received.

Monomers. Vinyl chloride obtained from Air Products Specialty Gas Division, C.P. grade, used as received. Vinyl acetate obtained from Monomer-Polymer Laboratories, used as received.

Polymerization Equipment

Fourteen liter stainless steel pressure reactor manufactured by Pressure Products Inc., Hatboro, Pa. Temperature control maintained at ± 0.1°C.

Polymerization Recipe and Procedure

(1) water 5000 g; (2) suspending agent 4.5 g; (3) sodium bicarbonate 4.5 g; (4) vinyl chloride and (5) vinyl acetate, 3000 g (total); (6) trichloroethylene, as indicated; (7) initiator (type and level), as indicated; (8) polymerization temperature, as indicated. Items 1, 2, 3, 5, 6, and 7 were added to the reactor under a nitrogen purge. The reactor was closed and pressure checked and then item 4 was added. The reactor was heated to the indicate temperature, usually requiring 12–15 min, and was held at isothermal conditions to a 95 psig pressure drop. In the experiments listed in Table II, the polymerizations were terminated at the indicated time.

Polymer Test Procedure

Inherent viscosity. ASTM Method D-1243-60A.

Melt flow. ASTM Method D-1238-57-T, condition at 175°C.

Bound vinyl acetate. infrared adsorption at 5.74 μm in 1,2-dichloroethylene solution.

Melt viscosity/elastic modulus/viscous modulus.

At 175°C in a Rheometrics Mechanical Spectrometer, measurements performed with a cone and plate apparatus.

RESULTS AND DISCUSSION

Bound Vinyl Acetate Content as a Function of Conversion under Different Polymerization Conditions

The effects of polymerization conditions on the bound vinyl acetate content of an 85/15 vinyl chloride/vinyl acetate copolymer were measured at different conversions. The experimental data detailed in Table II and Figure 1 show that over the experimental conditions studied the vinyl acetate content as a function of conversion was not affected by changes in polymerization temperature, initiator type and level, or the presence of tri-

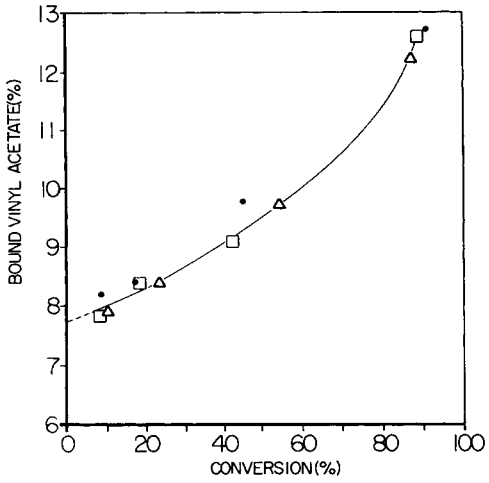

Fig. 1. Bound vinyl acetate level vs. conversion for different polymerization conditions. T_p (°C), TCE (phm): (●) 70,0; (□) T70, 0.366; (△) 65,0.

chloroethylene chain transfer agent. We observed that the molecular weight of the copolymer resin did increase with conversion as predicted by Cotman and co-workers.[13] In addition, we have shown that increasing the level of trichloroethylene has no effect on the vinyl acetate content at a fixed conversion (Table III). The decrease in the inherent viscosity is expected as is the increase in polymerization time; the trichloroethylene is a degradative chain transfer agent. The pseudochain transfer coefficient for trichloroethylene can be calculated for this particular system using methods previously developed.[14]

Reactivity Ratio for Vinyl Chloride–Vinyl Acetate

Using published reactivity ratio values for the vinyl chloride–vinyl acetate pair,[11] we have calculated the predicted composition as a function of conversion for an 85/15 comonomer mixture and compared it to the experimental data for composition vs. conversion from Table II. The results, shown in Figure 2, indicate that for these experimental conditions the published reactivity ratio data do not fit the experimental points. An alternative set of reactivity ratios was calculated from these data: R_1(VCM) = 2.47, R_2(VAc) = 1.99. This divergence between predicted values of 1.68/0.23 and experimental data may be due to a solubility of the vinyl acetate in the aqueous phase during the early stages of the polymerization or a water phase polymerization which becomes embedded in the polymer particles. These factors have not been explored.

Predictive Model for Bound Vinyl Acetate Levels

The vinyl acetate content of an 85/15 vinyl chloride/vinyl acetate copolymerization system has been shown to vary in a predictable manner with conversion and to be insensitive to a range of polymerization conditions. The copolymers prepared in the 4 × 4 matrix described in Table I

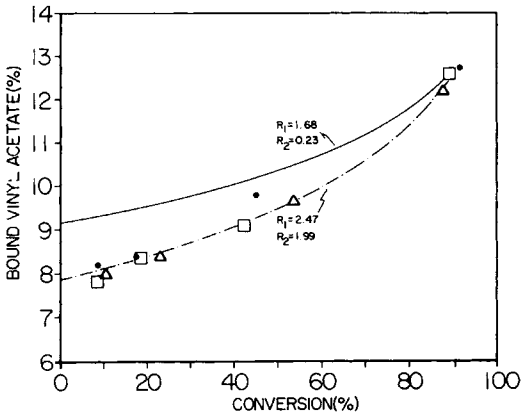

Fig. 2. Bound vinyl acetate level vs. conversion for 85/15 comonomer ratio. T_p (°C), TCE (phm): (●) 70,0; (□) T10, 0.366; (△) 65,0.

were all carried to a 95 psig pressure drop. The average conversion for these polymerizations is 86.5% with a standard deviation of ±2.3%. The bound vinyl acetate level for these 16 polymerizations can be modeled by a simple linear equation of the form

$$\text{VAcB} = K_1 + K_2[\text{VAcC}] \tag{1}$$

The constants for this equation are

$$K_1 = -0.39563$$

$$K_2 = 0.85094$$

$$R^2 = 0.996$$

Within the polymerization envelope described by the conditions in Table I approximately 85% of the charged vinyl acetate is incorporated into the copolymer. A comparison of the actual and predicted values for bound vinyl acetate level in these copolymers are noted in Table IV.

Predictive Model for Inherent Viscosity

The molecular weight of vinyl chloride homopolymer is controlled by the polymerization temperature[15] and the presence of chain transfer agents.[16] The polymerization temperature establishes the ratio of propagation constant (K_p) to monomer transfer constant (K_{trM}) for the reaction

$$M_1^{\bullet} + M_2 \xrightarrow{k_p} M_1 - M_2^{\bullet}$$

$$M_1^{\bullet} + M_2 \xrightarrow{k_{trM}} M_1 + M_2^{\bullet}$$

TABLE IV
Actual vs. Predicted Bound Vinyl Acetate Level

Observation	Actual	Predicted	Residual
1	4.4	3.86	+0.58
2	3.8	3.86	−0.06
3	3.8	3.86	−0.06
4	3.8	3.86	−0.06
5	8.2	8.11	+0.09
6	8.0	8.11	−0.11
7	8.1	8.11	−0.01
8	8.1	8.11	−0.01
9	12.4	12.4	+0.0
10	12.1	12.4	−0.30
11	12.9	13.4	−0.50
12	12.9	13.4	−0.50
13	17.4	16.6	+0.80
14	16.7	16.6	+0.10
15	16.5	16.6	−0.10
16	16.8	16.6	+0.20

The molecular weight of the resin is established primarily by the polymerization temperature; chain transfer agents are needed to reduce the molecular weight of a resin at a given polymerization temperature if a lower molecular weight is needed than what can be achieved at that particular polymerization temperature. Ravey and Waterman[17] examined the effect of polymerization temperature on the molecular weight of poly(vinyl chloride). They found that there was a linear relationship between polymerization temperature and inherent viscosity. Kronman et al.[18] extended this work to copolymers of vinyl chloride–vinyl acetate using the bound level of vinyl acetate in the copolymer. We have shown, in eq. (1), that there is a relationship at a fixed conversion between the charged and bound vinyl acetate level in the copolymer. Therefore, we can use the charged vinyl acetate level in a linear equation which combines the approach of both Ravey and Waterman with Kronman et al. to model the inherent viscosity of a vinyl chloride—vinyl acetate copolymer as

$$\mathrm{IV} = K_1 + K_2[1/T_{\mathrm{abs}}] + K_3[\mathrm{TCE}] + K_4[\mathrm{VAcC}] \tag{2}$$

Using the 4 × 4 matrix described in Table I, a multiple linear regression analysis was developed for eq. (2) with constants of

$$K_1 = -3.868$$

$$K_2 = +1.540 \times 10^{+3}$$

$$K_3 = -6.632 \times 10^{-2}$$

$$K_4 = -4.873 \times 10^{-3}$$

$$R^2 = 0.994$$

TABLE V
Comparison of Actual and Predicted Values for Inherent Viscosity

Observation	Observed value	Predicted value	Residual
1	0.725	0.700	0.025
2	0.587	0.600	−0.013
3	0.501	0.503	−0.002
4	0.414	0.414	0.000
5	0.707	0.709	−0.002
6	0.609	0.608	0.001
7	0.495	0.507	−0.012
8	0.419	0.422	−0.003
9	0.716	0.720	−0.004
10	0.616	0.617	−0.001
11	0.492	0.489	0.003
12	0.410	0.410	0.000
13	0.730	0.731	−0.001
14	0.617	0.627	−0.010
15	0.489	0.477	0.012
16	0.401	0.395	0.006

A comparison of the actual and predicted values for inherent viscosity based on predictive eq. (2) is noted in Table V.

Graphical representations of the interaction between polymerization temperature and trichloroethylene level on the inherent viscosity of a 90/10 adn 85/15 vinyl chloride/vinyl acetate copolymer are shown in Figures 3 and 4, respectively. The data from the inherent viscosity model equation show that (in Fig. 3) a 90/10 copolymer resin with an inherent viscosity of 0.65 can be prepared under a combination of conditions: at high level trichloroethylene (0.196/HM) and a low polymerization temperature (54.9°C) or at a zero level of trichloroethylene and a high polymerization temperature (65.8°C). The choice of operating conditions described by line C in Figure 3 will be dictated by initiator kinetics, reactor heat transfer capacity,

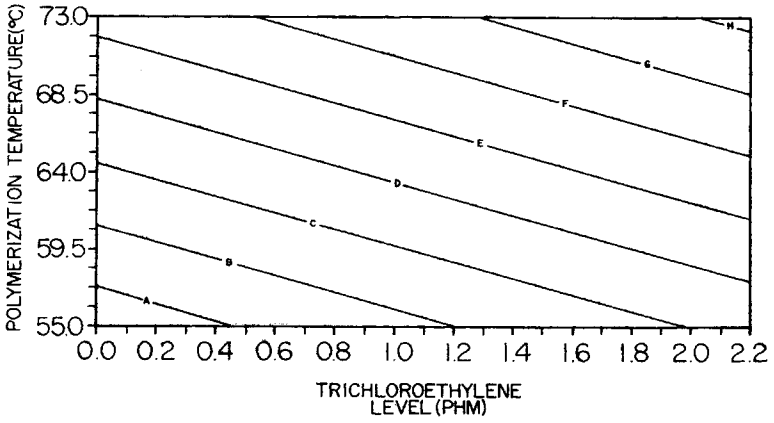

Fig. 3. Inherent viscosity contours for 90/10 vinyl chloride–vinyl acetate copolymers; polymerization temperature and trichloroethylene as process variables. Inherent viscosity (dL/g): (A) 0.75; (B) 0.70; (C) 0.65; (D) 0.60; (E) 0.55; (F) 0.50; (G) 0.45; (H) 0.40.

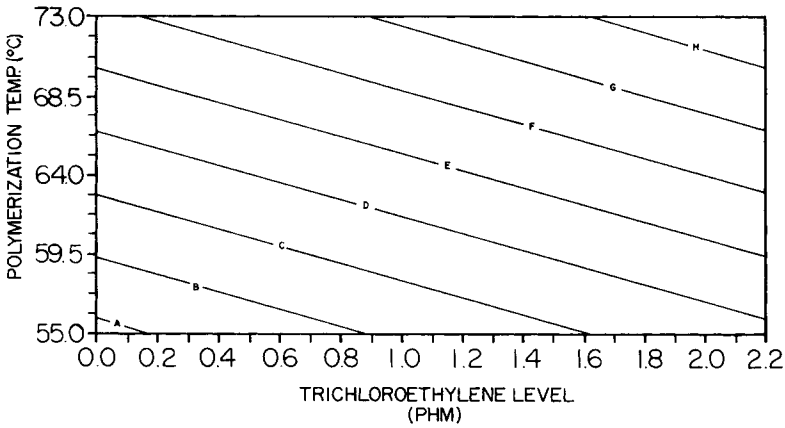

Fig. 4. Inherent viscosity contours for 85/15 vinyl chloride–vinyl acetate copolymers; polymerization temperature and trichloroethylene as process variables. Inherent viscosity (dL/g): (A) 0.75; (B) 0.70; (C) 0.65; (D) 0.60; (E) 0.55; (F) 0.50; (G) 0.45; (H) 0.40.

and the effect of trichloroethylene on resin properties. By comparison the inherent viscosity contours for the 85/15 copolymers (Fig. 4) are displaced toward lower temperatures/lower trichloroethylene levels, reflecting the higher chain transfer coefficient of the vinyl acetate monomer.

Predictive Models for Melt Rheological Properties

The melt rheology properties of vinyl chloride/vinyl acetate copolymers are controlled, in part, by the molecular weight of the polymer, the vinyl acetate content, and the presence of any long chain branch structures in the polymer chain. Rangnes[19] and Mondvai and co-workers[20] have developed master curves relating reduced viscosity to shear rate for vinyl chloride/vinyl acetate copolymers. Powell and Khanna[21,22] examined the effects of molecular weight and conversion sequence distribution on the rheological properties of vinyl chloride–vinyl acetate resins. Their work indicated that the elastic component of melt rheology for vinyl chloride/vinyl acetate copolymers may be controlled by varying the extent of branching in the resin. In a later work, Khanna[23] reviewed the effects of mixtures of resins on the melt viscosity/shear rate relationship and the experimental procedures needed to study audio record manufacturing. He indicated that a successful molding operation required a correct balance of melt viscosity and melt elasticity. The presence of low levels of vinyl acetate will have an effect on the mixing torque of a copolymer at 180°C. Tester[24] in a review of the technical literature shows that at a fixed molecular weight the equilibrium mixing torque of a series of vinyl chloride–vinyl acetate copolymers decreases in a nonlinear fashion as the VAcB level increases, with the first increment of VAcB being most effective in reducing the mixing torque. Veresova and co-workers[25,26] have examined the melt behavior of vinyl chloride/vinyl acetate copolymers in single screw extruders. They have developed empirical models which predict the length of the melt zone and the copolymer properties. These empirical models have not been extended to other melt rheological parameters for these copolymers.

The Tinius–Olsen melt index device is a simple capillary extrusion apparatus which is used extensively throughout the plastics industry to characterize the overall flow properties of resins and compounds. The device is designed to give a single point determination of melt flow rate at fixed shear rate and temperature. The primary purpose of this test is to determine qualitatively the flow rate between two different materials. By comparison the mechanical spectrometer can be used to determine the complex viscosity (η^*) as well as the elastic and viscous moduli (G' and G'') of polymeric materials. Both of these measurements can be used to develop a fundamental understanding of the effect of polymer structure on melt rheology and to compare quantitatively two different polymers.

Mathematical models can be formulated to simulate the relationship between independent and dependent parameters. These mathematical models can be based on established physical relationships; i.e., polymerization temperature and polymer inherent viscosity. Mathematical models can also be developed based on empirical relationships between the independent and dependent parameters, i.e., polymer inherent viscosity and Tinius–Olsen melt flow. The empirical models described in this publication were developed from linear regression procedures using linear, interactive, and higher-order terms. Our objective was to develop a series of models which could predict accurately the rheological properties of the copolymers using, as independent variables, either the polymerization parameters (i.e., T_p/VAcC/TCE) or copolymer parameters (i.e., VAcB/IV).

Tinius–Olsen Melt Flow

The Tinius–Olsen melt flow properties of these copolymers, as determined in the Tinius–Olsen device, represent a complex function of both elastic and viscous flow characteristics of the copolymer resin. The Tinius–Olsen melt flow data (Table I) cannot be separated into the various rheological components. Despite these limitations, we developed an empirical model to quantify the effects of either polymer structure as an independent variable base or polymerization conditions as an independent variable base on the Tinius–Olsen melt flow properties of the vinyl chloride/vinyl acetate copolymers. These models were based on an ln MF (ln melt flow) model which had already demonstrated its predictive effectiveness for vinyl chloride/propylene copolymers.[27]

Using standard linear regression techniques[28] a series of multiterm models based on inherent viscosity (IV) and bound vinyl acetate (VAcB) were tested as predictive equations of Tinius–Olsen melt flow (MF). The general form of the equations is described in Table VIA. In a sequence of steps the complexity of the model was increased from linear terms to interactive and square terms. The square of the correlation coefficient (R^2) increased with each additional level of terms. The $[IV]^2$ term was found to have a low F test factor of 0.4030, and deleting the $[IV]^2$ term had little effect on the R^2 value of Model 6A-4 which was the final form used for relating Tinius–Olsen melt flow to the polymer properties of IV and VAcB. A comparison of the predicted and actual melt flow values using model 6A-4 is noted in Table VII. The graphical representation for the Tinius–Olsen

TABLE VI
Predictive Models for Melt Flow

A. Using IV and VAcB

$$\ln MF = K_1 + K_2[IV] + K_3[VAcB] + K_4([VI] \cdot [VAcB] + K_5[IV]^2 + K_6[VAcB]^2$$

	Model	R^2
6A-1	$K_1 + K_2[IV] + K_3[VAcB]$	0.961
6A-2	$K_1 + K_2[IV] + K_3[VAcB] + K_4([IV] \cdot [VAcB]$	0.985
6A-3	$K_1 + K_2[IV] + K_3[VAcB] + K_4([IV] \cdot [VAcB] + K_5[IV]^2 + K_6[VAcB]^2$	0.995
6A-4	$K_1 + K_2[IV] + K_3[VAcB] + K_4([IV] \cdot [VAcB] + K_5[VAcB]^2$	0.993

$K_1 = 11.962$, $K_2 = -20.590$, $K_3 = 1.0611 \times 10^{-1}$, $K_4 = 6.5834 \times 10^{-1}$, $K_5 = -1.4950 \times 10^{-2}$

B. Using 1/Tabs, TCE, and VAcC

$$\ln MF = K_1 + K_2\frac{1}{T_{abs}} + K_3[TCE] + K_4[VAc] + K_5([TCE] \times [VAcC]) + K_6[TCE]^2 + K_7[VAcC]^2$$

	Model	R^2
6-B-1	$K_1 + K_2\frac{1}{T_{abs}} + K_3[TCE] + K_4[VAcC]$	0.940
6-B-2	$K_1 + K_2\frac{1}{T_{abs}} + K_3[TCE] + K_4[VAcC] + K_5([TCE] \times [VAcC])$	0.958
6-B-3	$K_1 + K_2\frac{1}{T_{abs}} + K_3[TCE] + K_4[VAcC] + K_5([TCE] \times [VAcC] + K_6[TCE]^2 + K_7[VAcC]^2$	0.993

$K_1 = 46.539$, $K_2 = -16.502 \times 10^{+3}$, $K_3 = 3.3606$, $K_4 = 5.4813 \times 10^{-1}$, $K_5 = -9.7836 \times 10^{-2}$, $K_6 = -6.0817 \times 10^{-1}$, $K_7 = -1.2022 \times 10^{-2}$

melt flow model (6A-4) is shown in Figure 5. The contour plot of melt flow as a function of IV and VAcB indicates the interaction between polymer molecular weight and polymer composition on the melt flow of these resins.

TABLE VII
Actual and Predicted Tinius–Olsen Melt Flow Data

Resin no.	Actual	Predictive eq. 6A-4	Residuals	Predictive eq. 6B-3	Residuals
1	0.600	0.618	− 0.018	0.808	− 0.208
2	2.60	3.76	− 1.16	2.36	0.24
3	29.0	21.7	7.3	27.3	1.7
4	109.	108.	− 1.	106.	3.0
5	3.40	2.78	0.62	3.54	− 0.14
6	14.0	13.1	0.90	10.5	3.5
7	65.0	61.1	3.9	56.8	8.2
8	210.	223.	−13.	227.	−17.0
9	8.00	7.54	0.46	8.34	− 0.34
10	26.0	27.3	− 1.3	25.2	0.8
11	118.	140.	−22.	145.	−25.0
12	303.	355.	−52.	354.	−51.0
13	11.6	12.7	− 0.9	10.8	0.8
14	36.0	34.8	1.2	33.1	2.9
15	151.	147.	4.0	179.	−28.0
16	388.	325.	63.0	324.	64.0

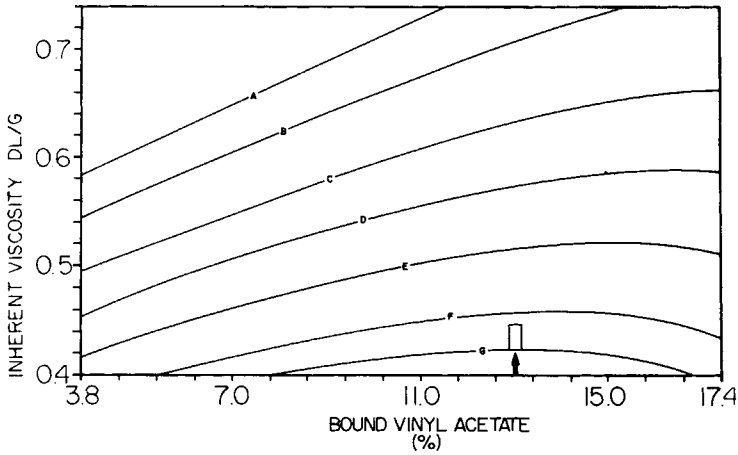

Fig. 5. Melt flow contour for vinyl chloride/vinyl acetate copolymers (g melt flow/10 min at 175°C): (A) 5; (B) 10; (C) 25; (D) 50; (E) 100; (F) 200; (G) 300.

The decrease in melt flow for the 200 melt flow contour at high VAcB levels may be experimental evidence for the chain entanglement effects of the vinyl acetate branch points in the low molecular weight resins. The contour plot indicates that a 100 melt flow resin (line F) can be achieved with a resin with 3.8% VAcB and an IV of 0.42 or with a resin with 13.0% VAcB and an IV of 0.50. While the Tinius–Olsen melt flow properties are identical, the elastic and viscous moduli, discussed in the next section, will be different for these resins.

Figure 5 can also be used to demonstrate the effects of variations in IV on the melt flow of a resin at a fixed VAcB level. For a resin with a VAcB of 13.0% (arrow in Fig. 5) the variation of IV from 0.42 to 0.44 represents a change in melt flow of 310 to 240, respectively.

A linear regression technique was also used to develop a predictive equation relating MF to the polymerization condition (i.e., T_{abs}/TCE/VAcC). The evaluation of this model from linear to interactive and square terms is described in Table VIB along with the R^2 values for each model. The highest order model (6B-3) was used for predicting MF based on polymerization conditions. A comparison of the actual and predicted values of MF based on Model 6B-3 is also noted in Table VII. Figure 6 indicates the range of polymerization temperature and trichloroethylene level that can be used to prepare a fixed melt flow resin for a comonomer composition of 90/10 vinyl chloride–vinyl acetate. Again, the choice of polymerization conditions will be dictated, in part, by the processing equipment and the effects of process conditions on the polymer particle morphology.

These results indicate that the Tinius–Olsen melt flow for vinyl chloride/vinyl acetate copolymers in this experimental space can be predicted successfully from a linear model based on either the polymer properties or the polymerization conditions.

Predictive equations 6A-4 and 6B-3 can be used to determine the effects of either copolymer structure or polymerization conditions on the Tinius–Olsen melt flow. Increasing the copolymer IV (molecular weight) will, as

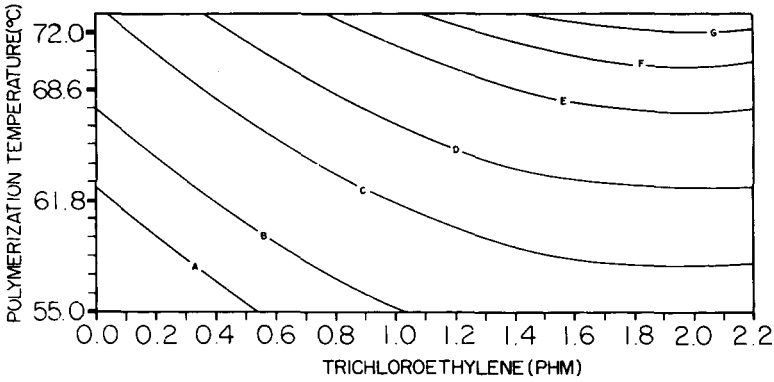

Fig. 6. Tinius–Olsen melt flow for 90/10 vinyl chloride/vinyl acetate copolymerization (g melt flow/10 min at 175°C): (A) 5; (B) 10; (C) 25; (D) 50; (E) 100; (F) 150; (G) 200.

expected, reduce the melt flow. The bound vinyl acetate level has a dual effect on melt flow; in term 3 (6A-4) it increases the melt flow by reducing the chain–chain interaction while in term 5 it decreases the melt flow by what may be experimental evidence for long chain branch entanglement. The presence of repeat units which disrupt the chain–chain interaction has been observed for styrene–butadiene systems[29] and polyvinylacetate.[30] In both polymer systems the introduction of a comonomer repeat unit which disrupts the chain–chain interaction reduces the melt viscosity of the polymer. In the case of styrene–butadiene copolymer, it is the presence of the butadiene which disrupts the styrene–styrene interactions. In the case of polyvinylacetate it is the presence of the branches which reduces the ability of chains to fully interact.

The effects of polymerization conditions on melt flow are illustrated in predictive equation 6B-6. Increasing the polymerization temperature (T_{abs}) will, as expected, increase the melt flow of the copolymer. The effects of TCE and VAcC on the melt flow of copoymer are, as with the VAcB, dual in nature. The TCE and VAcC, as first-order terms, increase the melt flow by reducing the molecular weight of the copolymer. As higher-order and interactive terms are added in model 6B-3, the TCE and VAcC terms reduce the melt flow of these copolymers by what we feel may be chain entanglement interactions.

The effects of variations in TCE and VAcC on melt flow of these copolymers are depicted in Figure 7 for a fixed polymerization temperature of 65°C. The data indicates the sensitivity of the Tinius–Olsen melt flow property to small changes in the TCE and VAcC levels and, as such, can be used to control the melt flow characteristics of these copolymers.

Elastic Modulus, Viscous Modulus, and Complex Viscosity

The melt rheological properties of the sixteen experimental resins were measured in a Rheometrics Mechanical Spectrometer. Elastic modulus (G') and viscous modulus (G'') were measured at 175°C using a cone and plate viscometer attachment. The complex viscosity (η^*) and loss tangent (tan δ)

TABLE VIII
Mechanical Spectrometer Data at 175°C

Resin no.	Dynamic oscillation frequency (rad/s)							
	10^{-1}				10^{0}			
	G'[a]	G''[b]	tan δ[c]	η^*[d]	G'[a]	G''[b]	tan δ[c]	η^*[d]
1	$4.04 \times 10^{+5}$	$2.30 \times 10^{+5}$	0.57	$4.65 \times 10^{+6}$	$8.64 \times 10^{+5}$	$5.13 \times 10^{+5}$	0.59	$1.01 \times 10^{+6}$
2	$5.42 \times 10^{+4}$	$6.35 \times 10^{+4}$	1.17	$8.35 \times 10^{+5}$	$1.96 \times 10^{+5}$	$2.53 \times 10^{+5}$	1.29	$3.20 \times 10^{+5}$
3	$4.07 \times 10^{+3}$	$9.02 \times 10^{+3}$	2.22	$9.90 \times 10^{+4}$	$1.96 \times 10^{+4}$	$4.43 \times 10^{+4}$	2.26	$4.84 \times 10^{+4}$
4	$6.48 \times 10^{+2}$	$3.15 \times 10^{+3}$	4.86	$3.22 \times 10^{+4}$	$5.03 \times 10^{+3}$	$1.49 \times 10^{+4}$	2.96	$1.57 \times 10^{+4}$
5	$1.17 \times 10^{+5}$	$1.27 \times 10^{+5}$	1.09	$1.73 \times 10^{+6}$	$3.99 \times 10^{+5}$	$4.07 \times 10^{+5}$	1.02	$5.70 \times 10^{+5}$
6	$2.65 \times 10^{+4}$	$4.10 \times 10^{+4}$	1.55	$4.88 \times 10^{+5}$	$1.20 \times 10^{+5}$	$1.78 \times 10^{+5}$	1.48	$2.14 \times 10^{+5}$
7	$4.55 \times 10^{+3}$	$1.14 \times 10^{+4}$	2.51	$1.23 \times 10^{+5}$	$2.44 \times 10^{+4}$	$6.55 \times 10^{+4}$	2.68	$6.99 \times 10^{+4}$
8	$1.19 \times 10^{+2}$	$1.44 \times 10^{+3}$	12.1	$1.44 \times 10^{+4}$	$1.68 \times 10^{+3}$	$1.08 \times 10^{+4}$	6.41	$1.09 \times 10^{+4}$
9	$2.81 \times 10^{+4}$	$5.63 \times 10^{+4}$	2.00	$6.29 \times 10^{+5}$	$1.59 \times 10^{+5}$	$2.54 \times 10^{+5}$	1.60	$3.00 \times 10^{+5}$
10	$5.97 \times 10^{+3}$	$2.16 \times 10^{+4}$	3.62	$2.24 \times 10^{+5}$	$5.39 \times 10^{+4}$	$1.39 \times 10^{+5}$	2.58	$1.49 \times 10^{+5}$
11	$6.21 \times 10^{+2}$	$5.03 \times 10^{+3}$	8.10	$5.07 \times 10^{+4}$	$8.03 \times 10^{+3}$	$3.18 \times 10^{+4}$	8.15	$3.2 \times 10^{+4}$
12	$9.52 \times 10^{+4}$	$1.82 \times 10^{+3}$	19.1	$1.82 \times 10^{+4}$	$1.01 \times 10^{+3}$	$1.15 \times 10^{+4}$	11.5	$1.15 \times 10^{+4}$
13	$2.86 \times 10^{+3}$	$1.79 \times 10^{+4}$	6.25	$1.81 \times 10^{+5}$	$3.85 \times 10^{+4}$	$1.19 \times 10^{+5}$	3.09	$1.25 \times 10^{+5}$
14	$7.46 \times 10^{+2}$	$5.26 \times 10^{+3}$	7.05	$5.31 \times 10^{+4}$	$6.81 \times 10^{+3}$	$4.09 \times 10^{+4}$	6.01	$4.15 \times 10^{+4}$
15	$1.11 \times 10^{+2}$	$7.02 \times 10^{+2}$	6.32	$7.11 \times 10^{+3}$	$9.79 \times 10^{+2}$	$1.29 \times 10^{+4}$	13.2	$1.28 \times 10^{+4}$
16	—	—	—	—	—	—	—	—
17[e]	$1.04 \times 10^{+6}$	$3.32 \times 10^{+5}$	0.32	$1.09 \times 10^{+7}$	$1.65 \times 10^{+6}$	$5.11 \times 10^{+5}$	0.31	$1.72 \times 10^{+6}$

1	$1.92 \times 10^{+6}$	$1.10 \times 10^{+6}$	0.57	$2.21 \times 10^{+5}$	$4.04 \times 10^{+6}$	$1.95 \times 10^{+6}$	0.48	$4.48 \times 10^{+4}$
2	$7.80 \times 10^{+5}$	$9.01 \times 10^{+5}$	1.15	$1.20 \times 10^{+5}$	$2.83 \times 10^{+6}$	$2.32 \times 10^{+6}$	0.82	$3.65 \times 10^{+4}$
3	$1.17 \times 10^{+5}$	$2.41 \times 10^{+5}$	2.05	$3.03 \times 10^{+4}$	$7.42 \times 10^{+4}$	$1.01 \times 10^{+6}$	1.36	$1.25 \times 10^{+4}$
4	$4.03 \times 10^{+4}$	$1.05 \times 10^{+5}$	2.61	$1.13 \times 10^{+4}$	$2.79 \times 10^{+5}$	$5.66 \times 10^{+5}$	2.03	$6.31 \times 10^{+3}$
5	$1.34 \times 10^{+6}$	$1.12 \times 10^{+6}$	0.84	$1.74 \times 10^{+5}$	$3.71 \times 10^{+6}$	$2.15 \times 10^{+6}$	0.58	$4.29 \times 10^{+4}$
6	$5.66 \times 10^{+5}$	$6.72 \times 10^{+5}$	1.19	$8.78 \times 10^{+4}$	$2.14 \times 10^{+6}$	$1.68 \times 10^{+6}$	0.79	$2.72 \times 10^{+4}$
7	$1.81 \times 10^{+5}$	$3.57 \times 10^{+5}$	1.97	$4.00 \times 10^{+4}$	$1.09 \times 10^{+6}$	$1.28 \times 10^{+6}$	1.17	$1.68 \times 10^{+4}$
8	$1.48 \times 10^{+4}$	$7.89 \times 10^{+4}$	5.29	$8.03 \times 10^{+3}$	$2.01 \times 10^{+5}$	$4.83 \times 10^{+5}$	2.40	$5.23 \times 10^{+3}$
9	$8.09 \times 10^{+5}$	$8.84 \times 10^{+5}$	1.09	$1.20 \times 10^{+5}$	$2.77 \times 10^{+6}$	$1.85 \times 10^{+6}$	0.67	$3.33 \times 10^{+4}$
10	$4.16 \times 10^{+5}$	$6.51 \times 10^{+5}$	1.57	$7.72 \times 10^{+4}$	$2.04 \times 10^{+6}$	$1.81 \times 10^{+6}$	0.89	$2.72 \times 10^{+4}$
11	$7.14 \times 10^{+4}$	$2.29 \times 10^{+5}$	3.21	$2.40 \times 10^{+4}$	$7.09 \times 10^{+5}$	$1.06 \times 10^{+4}$	1.50	$1.27 \times 10^{+4}$
12	$1.71 \times 10^{+4}$	$9.62 \times 10^{+4}$	5.62	$9.77 \times 10^{+3}$	$2.60 \times 10^{+5}$	$5.94 \times 10^{+5}$	2.28	$6.48 \times 10^{+3}$
13	$3.57 \times 10^{+5}$	$5.84 \times 10^{+5}$	1.64	$6.85 \times 10^{+4}$	$1.76 \times 10^{+6}$	$1.55 \times 10^{+6}$	0.88	$2.34 \times 10^{+4}$
14	$1.05 \times 10^{+5}$	$2.75 \times 10^{+5}$	2.62	$2.94 \times 10^{+4}$	$7.82 \times 10^{+5}$	$9.77 \times 10^{+5}$	1.25	$1.25 \times 10^{+4}$
15	$2.02 \times 10^{+4}$	$1.13 \times 10^{+5}$	5.50	$1.15 \times 10^{+4}$	$3.22 \times 10^{+5}$	$6.68 \times 10^{+5}$	2.07	$7.42 \times 10^{+3}$
16	$3.40 \times 10^{+3}$	$3.11 \times 10^{+4}$	9.73	$3.13 \times 10^{+3}$	$6.82 \times 10^{+6}$	$2.45 \times 10^{+5}$	3.59	$2.54 \times 10^{+3}$
17[e]	$2.62 \times 10^{+6}$	$8.29 \times 10^{+5}$	0.32	$2.74 \times 10^{+5}$	$4.14 \times 10^{+6}$	$1.16 \times 10^{+3}$	0.28	$4.30 \times 10^{+4}$

[a] G' = elastic modulus (dyn/cm^2).
[b] G'' = viscous modulus (dyn/cm^2).
[c] $\tan \delta = G''/G'$ = loss factor.
[d] η^* = complex viscosity (P).
[e] 17: Homopolymer resin IV = 0.717; $M_w/M_n = 2.19$.

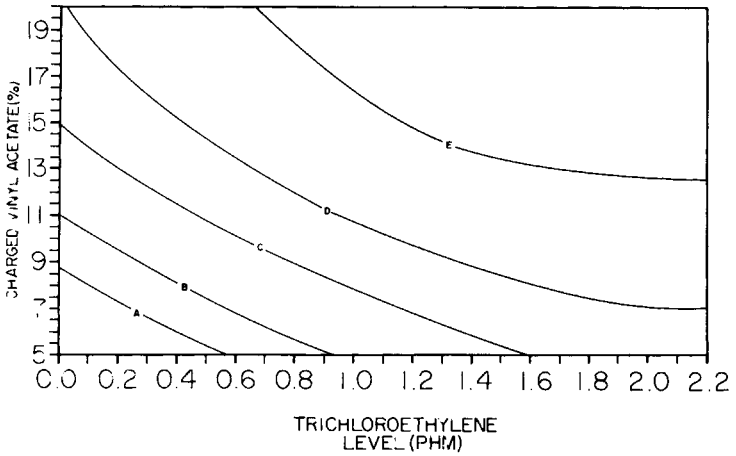

Fig. 7. Melt flow contours for vinyl acetate copolymer polymerized at 65°C (g melt flow/10 min at 175°C): (A) 5; (B) 10; (C) 25; (D) 50; (E) 100.

were calculated directly from G' and G'' at each of the dynamic oscillation frequencies. The general relationships of

$$\eta^* = \frac{[(G'')^2 + (G')^2]^{1/2}}{w} \tag{3}$$

and

$$\tan \delta = G''/G' \tag{4}$$

were used. A dynamic oscillation frequency (w) range of 10^{-1}–10^{+2} rad/s was used in this study. The mechanical spectrometer data are detailed in Table VIII. At each IV range the loss factor, tan δ, increases as the VAcB level increases. The tan δ for any vinyl chloride/vinyl acetate copolymer composition increases as the molecular weight decreases. These changes in tan δ represent the effects of both chain branching and the presence of vinyl acetate units in the copolymer main chains. These branch sites disrupt the chain–chain interactions of the vinyl chloride groups and reduce the melt viscosity of the copolymer. This effect has also been observed for propylene/vinyl chloride copolymers.[27] As either the vinyl acetate content is increased or as the copolymer molecular weight is decreased, the elastic modulus becomes an important component in the complex viscosity.

A comparison of the melt properties of resin 4 and resin 11 illustrates the difficulty associated with using Tinius–Olsen melt flow properties as a criteria for processibility over a wide range of oscillation frequency conditions. Resin 11 represents a typical primary phonograph record resin (12.9% VAcB; 0.492 IV). The elastic modulus becomes significant at high dynamic oscillation frequencies due to the chain branching sites associated with the vinyl acetate units in the main chain. By contrast, resin 4 (3.8% VAcB; 0.414 IV) exhibits a very narrow range of tan δ, indicating that the

elastic modulus does not become important over the dynamic oscillation frequency range being studied. A comparison of the elastic and viscous moduli, tan δ and complex viscosity for these two resins over the oscillation frequency range of 10^{-1}–10^{+2} rad/s is detailed in Table IX and Figure 8. Resin 11 exhibits a very wide range in tan δ over the shear rate range, indicating a significant elastic effect at high dynamic oscillation frequencies. By comparison resin 4 has a narrower range of tan δ values, indicating less of a shift to elastic flow properties. In addition, resin 4 exhibits lower complex viscosity values over the entire dynamic oscillation frequency range. These data indicate that the melt rheological properties of resin 4 would offer distinct advantages over resin 11 in compression-molding fabrication processes where configurations lead to variable shear rates on mold-filling operations.

At a fixed value of inherent viscosity (~0.71 dL/g), the relationship between the rheological properties of the complex viscosity (η^*) and the loss tangent (tan δ) and the polymer property of VAcB was examined using a commercial low molecular weight homopolymer (Air Products 1185 grade; IV = 0.717; M_w/M_n = 2.19). The G', G'', tan δ, and η^* values over the test range of dynamic oscillation frequencies are also noted in Table VIII for this homopolymer. Graphical representations of η^* vs VAcB (Fig. 9) and tan δ vs. VAcB (Fig. 10) indicate that the complex viscosity and tan δ relationship can be extended to the homopolymer (or 0% VAcB). The transition from a polymer with a highly elastic melt (homopolymer) to one with a predominantly viscous melt (17.4% VAcB) is related to the introduction of vinyl acetate units which disrupt the chain–chain interactions. As the level of vinyl acetate groups is increased, the elasticity effects of the chain–chain interactions are significantly reduced. This decrease in chain–chain interaction due to the presence of vinyl acetate groups also accounts for the decrease in complex viscosity for copolymer resin with increasing levels of VAcB.

Employing the same linear regression techniques as earlier described for the modeling of the Tinius–Olsen melt flow characteristics (the previous subsection), a series of multiterm models based on the polymer properties of inherent viscosity and bound vinyl acetate were tested as predictive equations for viscous modulus (G'') elastic modulus (G') and complex viscosity (η^*) at a dynamic oscillation frequency of 10^1 rad/s. Similar equations were developed for the rheological data at higher and lower dynamic oscillation frequencies. The general forms of the linear models examined are detailed in Table X. In each of the three models detailed in Table X, the components of the respective model were increased from linear to interactive and square terms. The R^2 value for the equation as well as the F test factor for each term was measured. The interactive term [IV][VAcB] was found to be insignificant for all of the rheological models and was deleted in the final form of these models because of the low F test factors. The final forms of the ln G', ln G'', and ln η^* models (Table X) are used to compare the actual and predicted values for the viscous and elastic moduli and complex viscosity. These comparative data are detailed in Tables XI, XII, and XIII, respectively.

TABLE IX
Comparison of Resins 11 and 4

	Resin 11	Resin 4
IV (dL/g)	0.492	0.414
VAcB (%)	12.9	3.8
MF (g/10 min)	118	109
tan δ at dynamic oscillation frequencies of		
10^{-1}	8.10	4.86
10^{0}	8.15	2.96
10^{+1}	3.21	2.61
10^{+2}	1.50	2.03
η^* P ($\times 10^{+4}$) at dynamic oscillation frequencies of		
10^{-1}	5.07	3.22
10^{0}	3.20	1.57
10^{+1}	2.40	1.13
10^{+2}	1.27	0.63

The general form of the predictive model

$$\ln(\text{property}) = K_1 + K_2[\text{IV}] + K_3[\text{VAcB}] - K_4[\text{IV}]^2 - K_5[\text{VAcB}]^2$$

was observed to be similar for G', G'', and η^*. The higher order terms, $[\text{IV}]^2$ and $[\text{VAcB}]^2$, are both negative, indicating an interaction which reduces the rheological property.

The polymerization properties of T_p, TCE, and VAcC were also used as the independent variables to model the rheological properties of G', G'',

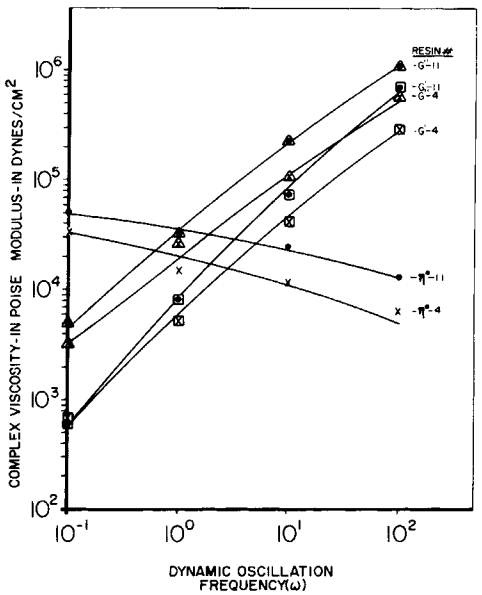

Fig. 8. Complex viscosity [(x) and (●)], elastic modulus [(⊠) and (⊡)], and viscous modulus [(◬) and (△)] as a function of dynamic oscillation frequency for resins 11 and 4, respectively.

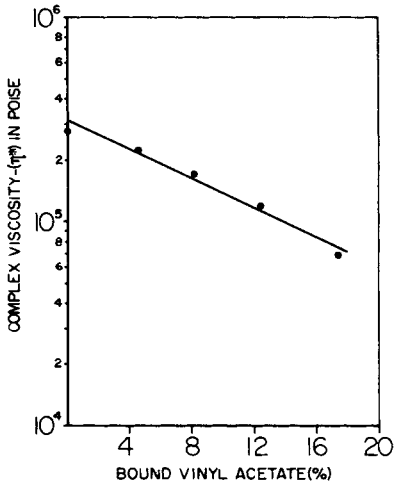

Fig. 9. Complex viscosity vs. bound vinyl acetate for IV = 0.71 at 10 rad/s.

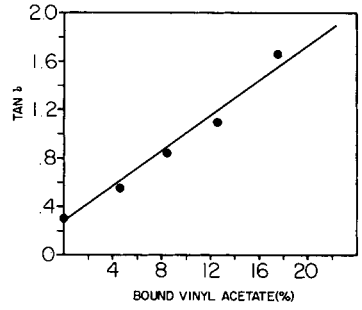

Fig. 10. Tan δ vs. bound vinyl acetate for IV = 0.71 at 10 rad/s.

TABLE X
Predictive Models for Melt Rheology Based on Polymer Properties[a]

Constant	Rheological property		
	G'	G''	η^*
K_1	− 2.8474	1.7886	4.5690×10^{-2}
K_2	41.921	31.188	29.568
K_3	9.3446×10^{-2}	1.1592×10^{-1}	8.3781×10^{-2}
K_4	−25.303	−20.525	−18.698
K_5	-1.1203×10^{-2}	-8.5724×10^{-2}	-8.0248×10^{-3}
R^2	.976	0.968	0.969

[a] $\ln(\text{property}) = K_1 + K_2[\text{IV}] + K_3[\text{VAcB}] + K_4[\text{IV}]^2 + K_5[\text{VAcB}]^2$.

TABLE XI
Actual and Predicted Values for Elastic Modulus (G') Dynamic Oscillation Frequency of 10^1 rad/s

Resin no.	Actual	Polymer model		Polymerization model	
		Predicted	Residual	Predicted	Residual
1	$1.92 \times 10^{+6}$	$1.61 \times 10^{+6}$	$0.31 \times 10^{+6}$	$1.99 \times 10^{+6}$	$-0.07 \times 10^{+6}$
2	$7.80 \times 10^{+5}$	$6.51 \times 10^{+5}$	$1.29 \times 10^{+5}$	$7.37 \times 10^{+5}$	$0.43 \times 10^{+5}$
3	$1.17 \times 10^{+5}$	$1.68 \times 10^{+5}$	$-0.51 \times 10^{+5}$	$1.55 \times 10^{+5}$	$-0.38 \times 10^{+5}$
4	$4.03 \times 10^{+4}$	$3.15 \times 10^{+4}$	$0.88 \times 10^{+4}$	$2.54 \times 10^{+4}$	$1.49 \times 10^{+4}$
5	$1.34 \times 10^{+6}$	$1.44 \times 10^{+6}$	$-0.10 \times 10^{+6}$	$1.57 \times 10^{+6}$	$-0.23 \times 10^{+6}$
6	$5.66 \times 10^{+5}$	$5.99 \times 10^{+5}$	$-0.33 \times 10^{+5}$	$5.73 \times 10^{+5}$	$-0.07 \times 10^{+5}$
7	$1.81 \times 10^{+5}$	$1.50 \times 10^{+5}$	$0.31 \times 10^{+5}$	$1.56 \times 10^{+5}$	$0.25 \times 10^{+5}$
8	$1.48 \times 10^{+4}$	$3.14 \times 10^{+4}$	$-1.66 \times 10^{+4}$	$2.77 \times 10^{+4}$	$-1.29 \times 10^{+4}$
9	$8.09 \times 10^{+5}$	$8.58 \times 10^{+5}$	$-0.49 \times 10^{+5}$	$8.63 \times 10^{+5}$	$-0.54 \times 10^{+5}$
10	$4.16 \times 10^{+5}$	$3.73 \times 10^{+5}$	$0.43 \times 10^{+5}$	$3.09 \times 10^{+5}$	$1.07 \times 10^{+5}$
11	$7.14 \times 10^{+4}$	$5.13 \times 10^{+4}$	$2.01 \times 10^{+4}$	$5.82 \times 10^{+4}$	$1.32 \times 10^{+4}$
12	$1.71 \times 10^{+4}$	$1.13 \times 10^{+4}$	$0.58 \times 10^{+4}$	$1.17 \times 10^{+4}$	$0.54 \times 10^{+4}$
13	$3.57 \times 10^{+5}$	$3.40 \times 10^{+5}$	$0.17 \times 10^{+5}$	$3.22 \times 10^{+5}$	$0.35 \times 10^{+5}$
14	$1.05 \times 10^{+5}$	$1.53 \times 10^{+5}$	$-0.48 \times 10^{+5}$	$1.13 \times 10^{+5}$	$-0.06 \times 10^{+5}$
15	$2.02 \times 10^{+4}$	$1.90 \times 10^{+4}$	$0.12 \times 10^{+4}$	$2.32 \times 10^{+4}$	$-0.30 \times 10^{+4}$
16	$3.40 \times 10^{+3}$	$3.71 \times 10^{+3}$	$-0.31 \times 10^{+3}$	$4.36 \times 10^{+3}$	$-0.96 \times 10^{+3}$

and η^*. The general form of the predictive model which simulated the rheological properties was

$$\ln(\text{property}) = K_1 + K_2(1/T_{\text{abs}}) + K_3\,[1/T_{\text{abs}}]\,[\text{TCE}] + K_4[\text{VAcC}]^2$$

In all of the forms of these models which we studied, the other combinations of interactive and higher order terms exceeded the F test criterion of 10% significance. The constants for each of the rheological model equations based on polymerization factors are detailed in Table XIV along with the R^2 value.

TABLE XII
Actual and Predicted Values for Viscous Modulus (G'') at Dynamic Oscillation Frequency of 10^1 rad/s

Resin no.	Actual	Polymer model		Polymerization model	
		Predicted	Residual	Predicted	Residual
1	$1.10 \times 10^{+6}$	$1.07 \times 10^{+6}$	$0.03 \times 10^{+6}$	$1.35 \times 10^{+6}$	$-0.25 \times 10^{+6}$
2	$9.01 \times 10^{+5}$	$6.80 \times 10^{+5}$	$2.21 \times 10^{+5}$	$7.95 \times 10^{+5}$	$1.06 \times 10^{+5}$
3	$2.41 \times 10^{+5}$	$2.96 \times 10^{+5}$	$-0.55 \times 10^{+5}$	$2.94 \times 10^{+5}$	$-0.53 \times 10^{+5}$
4	$1.05 \times 10^{+5}$	$0.98 \times 10^{+5}$	$0.07 \times 10^{+5}$	$8.69 \times 10^{+4}$	$0.18 \times 10^{+4}$
5	$1.12 \times 10^{+6}$	$1.15 \times 10^{+6}$	$-0.03 \times 10^{+6}$	$1.19 \times 10^{+6}$	$-0.07 \times 10^{+6}$
6	$6.72 \times 10^{+5}$	$7.57 \times 10^{+5}$	$-0.85 \times 10^{+5}$	$7.00 \times 10^{+5}$	$-0.28 \times 10^{+5}$
7	$3.57 \times 10^{+5}$	$3.27 \times 10^{+5}$	$0.30 \times 10^{+5}$	$3.22 \times 10^{+5}$	$0.35 \times 10^{+5}$
8	$7.89 \times 10^{+4}$	$1.17 \times 10^{+5}$	$-3.81 \times 10^{+4}$	$1.00 \times 10^{+5}$	$-2.11 \times 10^{+4}$
9	$8.84 \times 10^{+5}$	$9.15 \times 10^{+5}$	$-0.31 \times 10^{+5}$	$8.79 \times 10^{+5}$	$0.05 \times 10^{+5}$
10	$6.51 \times 10^{+5}$	$6.22 \times 10^{+5}$	$0.29 \times 10^{+5}$	$5.08 \times 10^{+5}$	$1.43 \times 10^{+5}$
11	$2.29 \times 10^{+5}$	$1.89 \times 10^{+5}$	$0.40 \times 10^{+5}$	$2.01 \times 10^{+5}$	$0.28 \times 10^{+5}$
12	$9.62 \times 10^{+4}$	$6.91 \times 10^{+4}$	$2.71 \times 10^{+4}$	$6.79 \times 10^{+4}$	$2.83 \times 10^{+5}$
13	$5.84 \times 10^{+5}$	$5.29 \times 10^{+5}$	$0.55 \times 10^{+5}$	$5.28 \times 10^{+5}$	$0.56 \times 10^{+5}$
14	$2.75 \times 10^{+5}$	$3.73 \times 10^{+5}$	$-0.98 \times 10^{+5}$	$3.02 \times 10^{+5}$	$-0.27 \times 10^{+5}$
15	$1.13 \times 10^{+5}$	$1.04 \times 10^{+5}$	$0.09 \times 10^{+5}$	$1.26 \times 10^{+5}$	$-0.13 \times 10^{+5}$
16	$3.11 \times 10^{+4}$	$3.50 \times 10^{+4}$	$-0.39 \times 10^{+4}$	$4.10 \times 10^{+4}$	$-0.99 \times 10^{+4}$

TABLE XIII
Actual and Predicted Values for Complex Viscosity (η^*) at Dynamic Oscillation Frequency of 10^1 rad/s

Resin no.	Actual	Polymer model		Polymerization model	
		Predicted	Residual	Predicted	Residual
1	$2.21 \times 10^{+5}$	$1.76 \times 10^{+5}$	$0.45 \times 10^{+5}$	$2.10 \times 10^{+5}$	$0.11 \times 10^{+5}$
2	$1.20 \times 10^{+5}$	$9.60 \times 10^{+4}$	$0.24 \times 10^{+5}$	$1.11 \times 10^{+5}$	$0.09 \times 10^{+5}$
3	$3.03 \times 10^{+4}$	$3.77 \times 10^{+4}$	$-0.74 \times 10^{+4}$	$3.68 \times 10^{+5}$	$-0.55 \times 10^{+5}$
4	$1.13 \times 10^{+4}$	$1.18 \times 10^{+4}$	$-0.05 \times 10^{+4}$	$0.976 \times 10^{+4}$	$0.15 \times 10^{+4}$
5	$1.74 \times 10^{+5}$	$1.74 \times 10^{+5}$	0	$1.80 \times 10^{+5}$	$-0.06 \times 10^{+5}$
6	$8.78 \times 10^{+4}$	$9.68 \times 10^{+4}$	$-0.90 \times 10^{+4}$	$9.50 \times 10^{+4}$	$-0.72 \times 10^{+4}$
7	$4.00 \times 10^{+4}$	$3.75 \times 10^{+4}$	$0.25 \times 10^{+4}$	$3.93 \times 10^{+4}$	$0.07 \times 10^{+4}$
8	$8.03 \times 10^{+3}$	$12.6 \times 10^{+3}$	$-4.57 \times 10^{+3}$	$11.0 \times 10^{+3}$	$-2.97 \times 10^{+3}$
9	$1.20 \times 10^{+5}$	$1.28 \times 10^{+5}$	$-0.08 \times 10^{+5}$	$1.23 \times 10^{+5}$	$-0.03 \times 10^{+5}$
10	$7.72 \times 10^{+4}$	$7.38 \times 10^{+4}$	$0.34 \times 10^{+4}$	$6.43 \times 10^{+4}$	$1.29 \times 10^{+4}$
11	$2.40 \times 10^{+4}$	$1.92 \times 10^{+4}$	$0.48 \times 10^{+4}$	$2.16 \times 10^{+4}$	$0.24 \times 10^{+4}$
12	$9.77 \times 10^{+3}$	$6.71 \times 10^{+3}$	$3.06 \times 10^{+3}$	$6.64 \times 10^{+3}$	$3.13 \times 10^{+3}$
13	$6.85 \times 10^{+4}$	$7.06 \times 10^{+4}$	$-0.21 \times 10^{+4}$	$6.61 \times 10^{+4}$	$0.24 \times 10^{+4}$
14	$2.94 \times 10^{+4}$	$4.19 \times 10^{+4}$	$-1.25 \times 10^{+4}$	$3.40 \times 10^{+4}$	$-0.46 \times 10^{+4}$
15	$1.15 \times 10^{+4}$	$0.999 \times 10^{+4}$	$0.15 \times 10^{+4}$	$1.23 \times 10^{+4}$	$-0.08 \times 10^{+4}$
16	$3.13 \times 10^{+3}$	$3.21 \times 10^{+3}$	$-0.08 \times 10^{+3}$	$3.58 \times 10^{+3}$	$-0.45 \times 10^{+3}$

A comparison of the actual and predicted values for G', G'', and η^* based on the polymerization models are also listed in Tables XI, XII, and XIII, respectively. The contour plot for η^* based on polymer properties of IV/VAcB (Fig. 11) indicates the sensitivity of complex viscosity to the molecular weight and bound vinyl acetate content of the resin. The complex viscosity exhibits a rather low sensitivity to the VAcB level over a wide range of compositions for the low molecular weight resin. As the molecular weight increases, the effects of the vinyl acetate groups become a more important factor in the complex viscosity. The effects of polymerization conditions (T_p/TCE/VAcC) on the complex viscosity are represented in Figure 12, where a series of iso(polymerization temperature) contour lines are displayed for a VAcC/TCE grid. Along each of these iso(polymerization temperature) lines a copolymer with an η^* of 15,000 P can be prepared. The combination of T_p/TCE/VAcC will dictate the IV and VAcB for that resin.

CONCLUSIONS

1. Predictive model equations have been elucidated for vinyl chloride–vinyl acetate copolymers of a composition range of 4–16% bound vinyl

TABLE XIV
Predictive Models for Melt Rheology Based on Polymerization Properties[a]

Constant	Rheological property		
	G'	G''	η^*
K_1	−31.027	−10.109	−16.626
K_2	$1.5339 \times 10^{+4}$	$8.1602 \times 10^{+3}$	$9.7283 \times 10^{+3}$
K_3	$-4.6683 \times 10^{+2}$	$-3.1480 \times 10^{+2}$	$-3.4305 \times 10^{+2}$
K_4	-7.6490×10^{-3}	-3.9897×10^{-2}	-4.8403×10^{-2}
R^2	0.978	0.971	0.982

[a] $\ln(\text{property}) = K_1 + K_2[1/T_{abs}] + K_3[1/T_{abs}]\,[\text{TCE}] + K_4[\text{VAcC}]^2$.

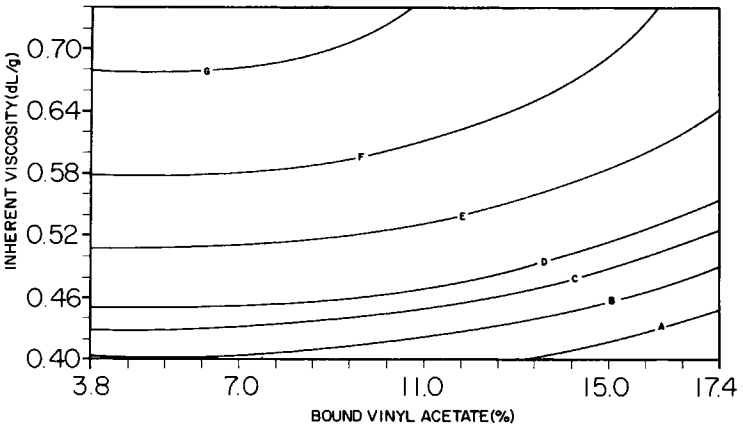

Fig. 11. Complex viscosity contours for vinyl chloride/vinyl acetate copolymers: (A) 6000; (B) 10,000; (C) 15,000; (D) 20,000; (E) 40,000; (F) 80,000; (G) 160,000.

acetate and an inherent viscosity range of 0.40–0.70 dL/g, which define the following properties:

The inherent viscosity of the copolymers can be predicted from the polymerization temperature, the initial level of charged vinyl acetate, and the trichloroethylene level. This model is based on the average chain transfer characteristics of the growing polymer chain to monomer and chain transfer agent during copolymerization.

The Tinius–Olsen melt flow of the copolymers can be predicted from both a polymerization condition model and a polymer physical properties model. Contour plots for isomelt flow conditions indicate the range of polymerization conditions or polymer properties over which a particular melt flow copolymer resin can be prepared. These two models indicate linear and interactive terms which control the Tinius–Olsen melt flow of the copolymer resins.

The elastic modulus, viscous modulus, and complex viscosity of the co-

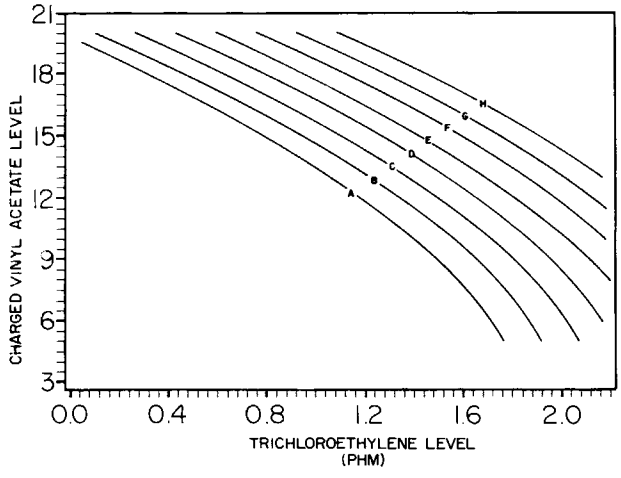

Fig. 12. Contour lines for complex viscosity = 15,000 P. Polymerization temperature (°C): (A) 73; (B) 71; (C) 69; (D) 67; (E) 65; (F) 63; (G) 61; (H) 59.

polymers can be predicted from either a polymerization condition model or a polymer properties model. Contour plots for isorheological properties indicated both the polymerization conditions or the copolymer properties needed to prepare resins with the same complex viscosity.

2. The bound vinyl acetate content of these copolymers affects their rheological properties; at high VAcB levels, the loss factor (tan δ) varies very widely as a function of shear rate changing the characteristics of the rheological properties from essentially viscous at low shear rate to a combination of viscous and elastic factors at high shear rate. By contrast a low vinyl acetate resin exhibits a rather narrow range in loss factor over a shear rate range of 10^{-1}–10^{+2} rad/s. This difference indicates that similarities in Tinius–Olsen melt flow properties for two widely different copolymers may not coincide with similar melt rheological properties over a wide dynamic oscillation frequency range.

3. At a molecular weight of about 0.71 IV, the tan δ and complex viscosity predictions were extrapolated successfully to the homopolymer. The tan δ relationship indicated that in the polymer melt the presence of vinyl acetate in the main chain reduces the chain–chain interaction and therefore shifts the complex viscosity from a highly elastic melt to a highly viscous melt.

4. The bound vinyl acetate level of these copolymers was not affected by the polymerization conditions used in the study. The copolymer composition as a function of conversion indicates that the reactivity ratios of the comonomers are R_1(VCM) = 2.47 and R_2(VAc) = 1.99. These reactivity ratios predict successfully the composition of the copolymer as a function of conversion. The bound vinyl acetate level of the copolymers, at a fixed pressure drop, could be predicted by a linear model based on the charged vinyl acetate level.

The authors wish to thank Mr. Stepen Stocker for the synthesis of these resins, Mr. Charles Johnson for the characterization measurements, and Mr. Tom Bzik for the modeling studies.

APPENDIX–NOMENCLATURE

G''	viscous modulus (dyn/cm^2)
G'	elastic modulus (dyn/cm^2)
IV	inherent viscosity (dL/g)
ln	natural log
M_w	weight-average molecular weight
M_n	number-average molecular weight
M_w/M_n	polydispersity factor
MF	melt flow (g/10 min at 75°C)
phm	per hundred of monomer
T_p	polymerization temperature (°C)
T_{abs}	polymerization temperature (K)
TCE	trichloroethylene level (%)
VAcC	vinyl acetate charged (%)
VAcB	vinyl acetate bound (%)
w	dynamic oscillation frequency (rad/s)
η^*	complex viscosity (P)
tan δ	loss tangent

References

1. M. Langsam, in *Encyclopedia of PVC,* 2nd ed., C. A. Heiberger and L. Nass, Eds., 1984, Marcel Dekker, New York, Chap. 3.

2. W. H. Starnes, F. C. Schilling, K. B. Abbas, R. E. Cais, and F. A. Bovey, Macromolecules, **12**, 556 (1979).

3. E. A. Collins and A. P. Metzger, *Polym. Eng. Sci.,* **10**, 57 (1970).

4. E. A. Collins and C. A. Daniels, *Polym. Eng. Sci.,* **14**, 357 (1974).

5. J. Lyngaae-Jorgensen, *Pure Appl. Chem.,* **53**, 509 (1981).

6. H. R. Chen and L. P. Blanchard, *J. Appl. Polym. Sci.,* **16**, 603 (1972).

7. J. Janca and M. Kolinsky, *J. Appl. Polym. Sci.,* **21**, 83 (1977).

8. J. Janca, L. Mrkvickova, M. Kolinsky, and A. S. Brar, *J. Appl. Polym. Sci.,* **22**, 2261 (1978).

9. J. Janca, S. Pokorny, and M. Kolinsky, *J. Appl. Polym. Sci.,* **23**, 1811 (1979).

10. S. Mori, *J. Chromatogr.,* **157**, 75 (1978).

11. F. R. Mayo, C. Walling, F. M. Lewis, and W. F. Hulse, *J. Am. Chem. Soc.,* **70**, 1532 (1948).

12. D. Stein and G. V. Schultz, *Makromol. Chem.,* **52**, 249 (1962).

13. J. D. Cotman, M. F. Gonzales, and G. C. Claver, *J. Polym. Sci., A-1,* **5**, 1137 (1967).

14. M. Langsam, *J. Appl. Polym. Sci.,* **23**, 867 (1979).

15. J. T. Barr, in *The Manufacture of Plastics,* W. M. Smith, Ed., Reinhold, New York, 1968, Chap. 7, p. 315.

16. C. Walling, *Free Radicals in Solution,* Wiley, New York, 1957, p. 159.

17. M. Ravey and J. A. Waterman, *J. Polym. Sci. Chem.,* **A-13**, 1475 (1975).

18. A. G. Kronman, B. I. Fedoseev, M. A. Chekushiua, L. I. Arknipova, and F. Lepaev, *Plast. Massy,* **7**, 48 (1976).

19. P. Rangnes, *Kunstoffe,* **51**, 428 (1961).

20. I. Mondvai, L. Halasz, and I. Molner, *Periodica Polytechnique,* **3**, 203 (1971).

21. E. Powell and S. K. Khanna, *Soc. Plast. Eng. J.,* **27**, 33 (1971).

22. S. K. Khanna and E. Powell, *J. Appl. Polym. Sci.,* **16**, 2013 (1972).

23. S. K. Khanna, *J. Audio Eng. Soc.,* **24**, 464 (1976).

24. D. A. Tester, in *Manufacturing and Processing of PVC,* R. H. Burges, Ed., Macmillan, New York, 1981, Chap. 9, p. 230.

25. G. N. Veresova, V. Yu. Kasankov, V. S. Kim, and N. I. Basov, *Plaste Kautsch.,* **24**, 199 (1977).

26. G. N. Veresova and V. S. Kim, *Plaste Kautsch.,* **25**, 241 (1978).

27. M. Langsam, *J. Appl. Polym. Sci.,* **21**, 1057 (1977).

28. G. E. P. Box, W. G. Hunter, and J. S. Hunter, *Statistics for Experimenters,* Wiley, New York, 1978.

29. G. Kraus and J. T. Gruver, *J. Appl. Polym. Sci.,* **11**, 2121 (1967).

30. W. W. Graessley and J. S. Prentice, *J. Polym. Sci.,* **A2-6**, 1887 (1968).

Received March 7, 1984
Accepted August 17, 1984